Systems & Control Transactions

Research Article - Peer Reviewed Conference Proceeding
ESCAPE 35 - European Symposium on Computer Aided Process Engineering
Ghent, Belgium. 6-9 July 2025
Jan F.M. Van Impe, Grégoire Léonard, Satyajeet S. Bhonsale,
Monika E. Polańska, Filip Logist (Eds.)

PSE PRESS

Robust pharmaceutical tableting process through combined probabilistic design space and flexibility analysis

Ashish Yewale[a], Xuming Yuan[a] and Brahim Benyahia[a]*

[a] Department of Chemical Engineering, Loughborough University, Leicestershire, UK
* Corresponding Author: b.benyahia@lboro.ac.uk

ABSTRACT

This study investigates the development of a probabilistic design space (DS) for a tableting process, focusing on the uncertainty in critical model parameters. A an empirical model is used to assess the impact of critical process parameters (CPPs), including lubrication extent and porosity, on tablet tensile strength (CQA). By incorporating Monte Carlo and Bayesian techniques, the uncertainty of five model parameters is propagated, allowing the estimation of feasibility probabilities for achieving CQAs with a reliability greater than 0.95. The resulting probabilistic DS provides manufacturers with a tool to assess the likelihood of meeting CQAs under varying production conditions. The findings indicate that specific combinations of lubrication rate and porosity define a robust DS within the acceptable operating region, ensuring consistent tableting performance even in the presence of uncertainties. This approach emphasizes the importance of probabilistic DS in optimizing manufacturing processes and delivering built-in quality assurance.

Keywords: Probabilistic design space, Tableting process, Bayesian inference, Operational flexibility, Acceptable Operating Region, Nominal Operating Point inference

1. INTRODUCTION

Pharmaceutical manufacturing operates under stringent regulatory constraints, requiring a thorough understanding of the interplay between raw material attributes, process parameters, and product quality[1–3]. To meet these requirements, Quality by design (QbD) has emerged as a key approach to achieve consistent, high-quality production by identifying critical material attributes (CMAs) and critical process parameters (CPPs) that impact critical quality attributes (CQAs). The International Council for Harmonization (ICH) introduced the QbD initiative through guidelines ICH Q8–12, emphasizing a scientific and risk-based approach over traditional quality-by-testing methods[4,5]. This transformation in pharmaceutical development has enabled the development of robust process designs through the concept of design space (DS), which allows for safe operation without the need for additional regulatory approvals. DS can be identified using various strategies, such as empirical models, data-driven models, response surface methodologies, multivariate experimental design, and high-dimensional model representation, all grounded in existing literature, prior experiences, and process knowledge. However, conventional DS models often assume constant model parameters, overlooking the inherent uncertainty in both model parameter and the manipulated variables[6]. By incorporating these uncertainties, which typically can be captured by probabilistic distributions, the DS evolves from a deterministic framework to a probabilistic DS. This transformation provides a more realistic and adaptable approach to ensuring consistent product quality under variable conditions.

Bayesian approaches have been used to identify probabilistic DSs, in various process such as spray drying processes[7], crystallization of casopitant mesylate[8], and solid oral dosage form[9]. The DS is a subset of the knowledge space, which represents the operating envelope explored, studied, and well understood. To effectively characterize the probabilistic DS, computational methods are crucial, particularly in addressing uncertainties within model parameters[10]. Sampling algorithms

method discretizes the model parameter space by generating samples that account for probabilistic distributions of uncertainties. Techniques such as uniform gridding or (quasi) Monte Carlo simulations are commonly employed to propagate uncertainty and ensure all quality constraints are met with the desired level of reliability. This sampling-based approach is particularly effective in capturing the complexities of probabilistic DS offering robust solution for compliance with quality requirements. As number of parameters increases, these sampling methods suffer from the "curse of dimensionality", making them computationally expensive. In addition, these methods distribute samples uniformly, wasting computational resource on low-probability regions while undersampling high-probability areas.

To address these challenges, a Monte Carlo technique based on nested sampling method was developed in conjunction with a Bayesian inference based parameter estimation. The algorithm works by progressively sampling within nested contours of increasing likelihood, maintaining a dense sample in high-likelihood regions. This adaptive approach helps overcome the limitations of traditional methods, allowing particularly the handling of multimodal posteriors and high-dimensional spaces. Additionally, it allows for flexible adjustment of feasibility probability thresholds to meet industrial reliability requirements. Nested sampling integrates seamlessly with Bayesian parameter estimation, providing a unified probabilistic approach to probabilistic DS characterization. Overall, nested sampling provides a more efficient, flexible, and accurate tool for ensuring robust product quality in pharmaceutical manufacturing.

2. METHOD

2.1 Case study: Tablet Lubrication process

Lubrication plays a critical role in tablet manufacturing, particularly in direct compression process, as it enhances tablet ejection during compression. However, the extent of lubrication must be carefully controlled, as it significantly impacts the overall quality and efficacy of the drug product. The interaction between lubrication and compression processes influences key quality attributes, such as tablet tensile strength. An increase in lubrication may lead to a reduction in tensile strength, a challenge that can potentially be mitigated by increasing compaction pressure.

Kushner and Moore (2010)[11] developed an empirical model to capture lubrication and compaction performance across various blending conditions and scales, given by:

$$\sigma = \sigma_{sf=0.85,0}\big((1-\beta)+\beta exp(-\gamma k)\big) \quad (1)$$

where $\sigma_{sf=0.85,0}$ is the initial tensile strength at 0.85 solid fraction, β is the total fraction of tensile strength that can be lost due to lubrication, and γ is the lubrication rate constant of the blend.

Based on this initial approach, Nassar et al. (2022)[12] proposed a simplified model that relates the Kushner model parameters ($\sigma_{sf=0.85,0}$, and β) with the porosity:

$$\sigma_{sf=0.85,0} = a_1 exp\big(b_1(1-sf)\big) \quad (2)$$

$$\beta = a_2(1-sf)+b_2 \quad (3)$$

This model involves five unknown parameters: $\theta = [a_1(MPa);\ b_1(-);\ a_2(-);\ b_2(-);\ \gamma(dm^{-1})]$ and captures the effects of solid fraction and lubrication extent on tablet tensile strength which are identified as CPPs, while tablet tensile strength is regarded as a CQA.

2.2 Bayesian parameter estimation

In this study, the uncertainty associated with model parameters (θ) is quantified using Bayesian inference. Experimental data published by Kushner et al. (2012)[13] for the Turbula mixer was utilized to estimate these parameters and identify the uncertainties in the model relationships. This dataset includes tensile strength measurements under varying conditions of lubrication and compaction, providing a reliable basis for parameter estimation.

Bayesian methods provide a powerful framework for parameter estimation, incorporating prior knowledge and experimental data to obtain a posterior distribution for each model parameter. This distribution provides the most likely values of the parameters and quantifies the associated uncertainty, which is crucial for model validation and identifying the robust design space.

Bayes' Theorem combines prior knowledge about the model parameters with the experimental data to update the probability distribution of the parameters. This approach is mathematically expressed as:

$$p(\theta|D) = \frac{\mathcal{L}(D|\theta)\varphi(\theta)}{P(D)} \quad (4)$$

Here, $\varphi(\theta)$ is the prior knowledge about the true value of the model parameters, $p(\theta|D)$ is the posterior distribution representing an updated belief about model parameter value after observing the experimental data. $\mathcal{L}(D|\theta)$ is likelihood distribution and $P(D)$ is marginal likelihood, which normalizes the posterior. The posterior distribution offers not only the most likely parameter values but also quantifies the uncertainty surrounding these estimates.

2.3 Nested sampling

The mathematical model describing the relationship between the CPPs, CMAs and CQAs is expressed as:

$$CQAs = f(x,\theta) \quad (5)$$

Here x represents the vector of CPPs within the knowledge domain (χ) in real space (R^s), while θ is the uncertain model parameter defined in m-dimensional real

space (R^m) with a probability density function (pdf).
The constraints on the CQAs, which can be combined with additional process constraints, are given as

$$G(x,\theta) := g(x, f(x,\theta)) \geq g^* \tag{6}$$

where g^* represents a vector of predefined bounds for the CQAs. If the uncertainty in the model parameter is disregarded, the nominal DS is designed as

$$DS_{nom} := \{x \in \chi | g(x, G(x,\theta_{nom})) \geq g^*\} \tag{7}$$

where θ_{nom} represents a specific nominal value of the model parameter. However, since θ is inherently uncertain, whether due to limitation in parameter estimation or to the nature of modeling and data, ignoring this uncertainty may lead to oversimplified DS representations.

To address this, a probabilistic DS is expressed as

$$DS = \{x \in \chi | E_\theta[p(CQAs \in \Lambda) | X = x, \theta] \geq \alpha\} \tag{8}$$

According to equation (8), the DS is a subset of the knowledge space (χ), mapping a set of CPPs (x) where the probability of CQAs satisfying the specified limit (Λ) exceeds a specified reliability value (α), while accounting for the uncertainty in the model parameter θ. The reliability value should be kept between $0 < \alpha \leq 1$.
A Bayesian framework addresses this challenge by treating θ as a random variable with joint probability distribution $p(\theta)$, representing the belief about its potential value of θ. For example, $p(\theta)$ can be estimated from experimental data using Bayesian inference. In this framework, the model is primarily used to predict the probability that the manufacturing process is feasible for a given set of conditions.

$$\mathbb{P}[G(x,\cdot) \geq g^* | p(\theta)] := \int_{\{\theta: G(x,\theta) \geq g^*\}} p(\theta) d\theta \tag{9}$$

Hence, the probabilistic DS can be presented as

$$DS = \left\{x \in \chi \middle| \left[\mathbb{P}[G(x,\cdot) \geq g^* | p(\theta)]\right] \geq \alpha\right\} \tag{10}$$

In general, at fixed manipulated variable $x,\cdot$ sampled from S_d, the probability of meeting CQA constraint is estimated via an ensemble of simulation over uncertainty scenario in S_θ.

$$\hat{\mathbb{P}}[G(x_i,\cdot) \geq g^* | S_\theta] := \sum_{(\theta_j,\omega_j)\epsilon S_\theta} \mathbb{I}\left[G\left(x_i,\theta_j\right)\right]\omega_j \tag{11}$$

where $\mathbb{I}[\cdot]$ is an indicator function, which takes the value 1 if the constraint is satisfied, and 0 if they are not satisfied. The model parameters θ_i with corresponding weights ω_i are sampled from the posterior distribution function $p(\cdot)$. This method requires running full model $N_d \times N_\theta$ times, where N_d and N_θ are the number of sample points taken from S_d and S_θ space, respectively, which can be exceedingly costly for practical test cases.

In Nested sampling, the posterior distribution $p(\theta)$ can be derived using Bayes' theorem, which was explained earlier. The equation for the posterior distribution in the context of nested sampling is:

$$\left.\begin{aligned} p(\theta) &= \frac{\mathcal{L}(\theta)\varphi(\theta)}{\mathrm{Z}} \\ \mathrm{Z} &:= \int \mathcal{L}(\theta)\varphi(\theta)\, d\theta \end{aligned}\right\} \tag{12}$$

where Z is referred to as the Bayesian evidence, and it represents the integral of the likelihood weighted by the prior. Unlike the traditional Markov Chain Monte Carlo (MCMC) methods, which aim primarily to approximate the posterior distribution $p(\theta)$, nested sampling focuses on directly estimating Z as its primary target. This is achieved by iteratively sampling within nested contours of increasing likelihood, ensuring a systematic exploration of the parameter space. As a result, regions of high likelihood are densely sampled, enabling accurate estimation of Z. This feature is particularly advantageous for Bayesian model selection, as the evidence Z quantifies the overall fit of a model to the data while accounting for model complexity.

To implement nested sampling in DS characterization, N_L points in the set of live points (S_L), can be initialized via uniform sampling in the design space. Nested sampling begins by estimating the feasibility probability at each of these points, according to equation (12), which calculates the likelihood of meeting the CQA constraints as described in equation (11). Estimating the feasibility probability for a given live point requires process model runs for the uncertainty set S_θ. The number of models run for N_θ parameters in the uncertainty set S_θ is a critical computational cost of the algorithm.

During each iteration, the worst point x, having the lowest feasibility probability, is identified. This point is determined by calculating minimum feasibility probability ($\hat{\mathbb{P}}_{min}$) across all the live points, as shown in equation (13):

$$\hat{\mathbb{P}}_{min} = min_i\left\{\hat{\mathbb{P}}[G(x_i,\cdot) \geq g^* | S_\theta] : i \in S_L\right\} \tag{13}$$

The corresponding live point x is the one that minimizes this probability is identified using equation (14), expressed as:

$$x = argmin_i\left\{\hat{\mathbb{P}}[G(x_i,\cdot) \geq g^* | S_\theta] : i \in S_L\right\} \tag{14}$$

Once the worst point is identified, it is replaced by a new point selected from the set of replacement point (N_R). To accelerate the process, the evaluation of a replacement candidate can be interrupted if the cumulative feasibility probability mass and the remaining samples are below a certain threshold. This strategy reduces unnecessary computations by rejecting unlikely candidates early. Rejected points are not added to the result set, ensuring that the focus remains on finding N_L points with feasibility probabilities greater than or equal to the target reliability (π).

The replaced live points, along with their associated feasibility probabilities, are then stored in the result set for further analysis. The main iteration concludes when all live points meet or exceed the target probability. These points are then added to the result set, which may

also include dead points. If multiple replacements occur during the final iteration, the result set may exceed N_L. Conversely, if the set of live points becomes empty, the algorithm stops prematurely. This situation can be detected by monitoring the rate of improvement in feasibility over several iterations, ensuring that the algorithm doesn't waste resources when progress slows, or the reliability threshold is set too high.

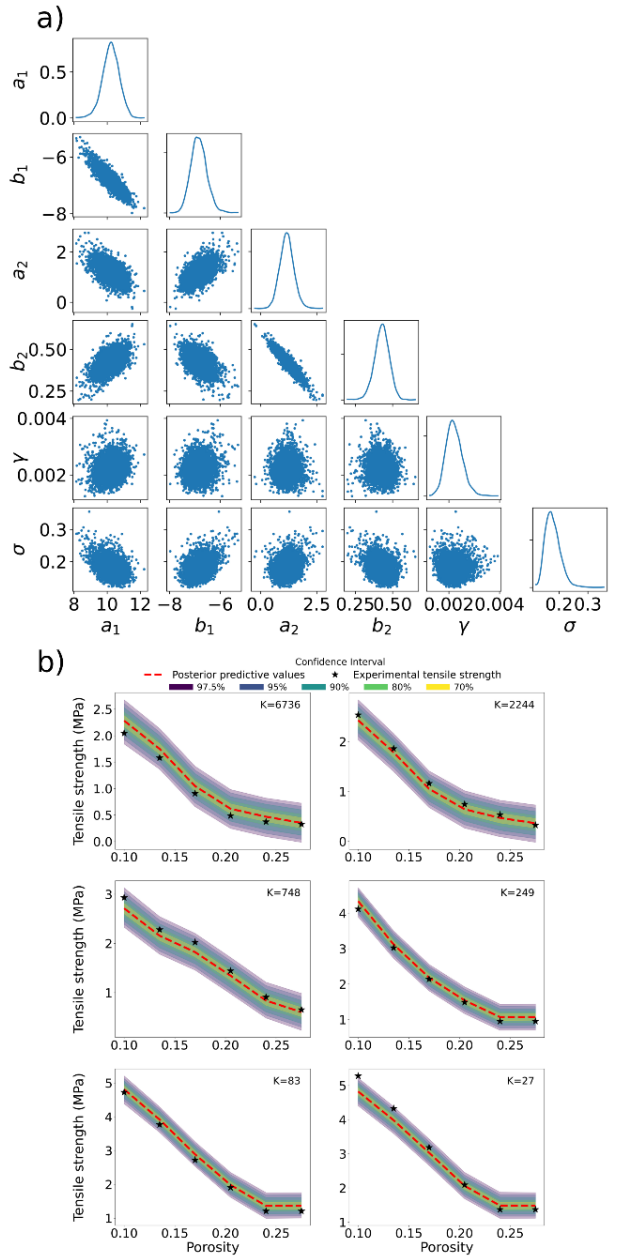

Figure 1. (a) Pair-wise plots of posterior distributions and (b) Model predictions with the confidence bands based on Bayesian inference.

The total number of process model runs (N_{total}), which is required for N_{iter} iterations of nested sampling, can be expressed as:

$$N_{total} = N_\theta(N_L + N_{iter}N_R) \quad (15)$$

where, N_L is total number of live points, N_R is total number of replacement points, and N_{iter} number of nested sampling iterations.

2.4 Flexibility Analysis and the Acceptable Operating Range (AOR)

The flexibility of a system is dictated by the size and shape of its Acceptable Operating Range (AOR) around the Nominal Operating Point (NOP). A larger AOR indicates greater flexibility, allowing the system to operate effectively across a wider range of conditions, while a smaller AOR reflects more constrained operating conditions, limiting the system's ability to adapt to variations[14]. The AOR is identified through a bisection search starting from a NOP and expanding uniformly in all directions until one of its vertices hits the boundary of the design space. The selection of points is entirely dependent on the constraints and nature of the problem. The algorithm terminates when either the maximum number of iterations is reached or when all vertices in the expansion are within the acceptable operating range, and the difference between the upper and lower bounds is smaller than the specified bisection tolerance. If the algorithm reaches the maximum number of iterations before convergence, it may indicate that the vertices haven't expanded sufficiently or the bisection tolerance hasn't been met, in which case increasing the number of iterations may help achieve better convergence.

3. RESULTS

The proposed Bayesian parameter estimation framework was implemented using experimental data from Kushner et al. (2012)[13] to quantify the uncertainties in the model parameters described in Sections 2.1 and 2.2. The pair-wise plot for all five model parameters ($\theta = [a_1, b_1, a_2, b_2, \gamma]$ constructed using the posterior samples obtained from Markov Chain Monte Carlo (MCMC), is illustrated in Figure 1(a). The plot shows the marginal posterior distributions along the diagonal as kernel density estimates and joint distributions of parameter pairs as contour plots below the diagonal. The sharpness of the marginal posterior probability density functions (PDFs), along with small coefficients of variation (CV), indicates that the parameter uncertainties are well quantified. The contour plots also provide key insights into the correlations between model parameter pairs [15], which are further explained by the Pearson correlation matrix in figure 2. For example, a strong negative correlation was observed between certain parameter pairs, such as a_1 & b_1, and a_2 & b_2. The covariance matrix, which captures these relationships, provides a more realistic measure of model uncertainty, as it reflects the actual behavior of the

system based on the posterior samples. Table 1 presents the sample mean, standard deviation, and CV values of the posterior MCMC samples. Furthermore, figure 1(b) shows the posterior predictive simulations (PPS), generated using the values of θ and σ obtained during the inference. The mechanistic model used for the PPS is the same as the one used for the inference, facilitating direct comparison with the "experimental" data. The PPS confidence ranges are shown by the colored areas in figure 1(b), while the "experimental" values are indicated by the black stars overlaid on the prediction plots.

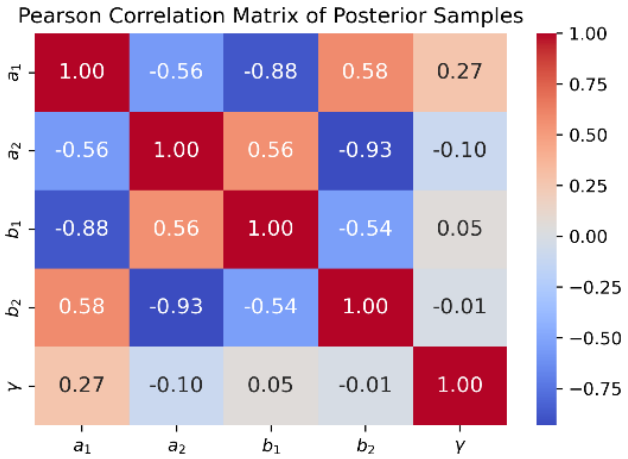

Figure 2. Pearson correlation matrix of model parameters. (Darker shades indicate stronger correlations).

Table 1. Summary of the Bayesian inference posterior statistics for all model parameters

Model parameter	Mean	Std deviation	coefficients of variation (CV)
a_1	10.2268	0.508	0.0497
b_1	-6.83272	0.3116	-0.045
a_2	1.1765	0.3126	0.265
b_2	0.4268	0.0492	0.115
γ	0.00222	0.00033	0.150

The knowledge space for this analysis is defined in terms of two CPPs: (i) the lubrication extent $k(dm^{-1}) \in [27, 7000]$, and (ii) porosity, $\mathcal{E} \in [0.01, 0.31]$. The feasible operating region is further constrained by the CQA limits for 8 mm flat faced tablets, $Ts(MPa) \in [2,\ 6]$, ensuring the tableting tensile strength delivers the required quality attributes. The CQA constraints provide essential constraints, limiting the parameter space and ensuring that the system remains within acceptable performance limits. Next, the impact of uncertainty is captured by the probabilistic design space by propagating the model parameter uncertainties, represented as a set of weighted samples $\{\theta_j, \omega_j\}_{j=1,\dots N_\theta}$.

A nested sampling algorithm with a reliability target value of α=0.95 is implemented to focus on higher likelihood samples. To ensure the sufficiently high sample density, 500 live points and 100 uncertainty model descriptions, each with equal weights, are drawn from the posterior density function. The resulting samples are depicted in different colors according to their reliability membership, providing a clear visualization of the probabilistic design space and highlighting areas of high and low reliability in figure 3. On comparison with quasi MCMC, it is observed that nested sampling method efficiently focusing on high-probability region of knowledge space and eliminate the least-probability sampling points. This targeted approach not only enhances the precision of the estimates but also significantly reduces the computational resources required compared to more exhaustive sampling methods.

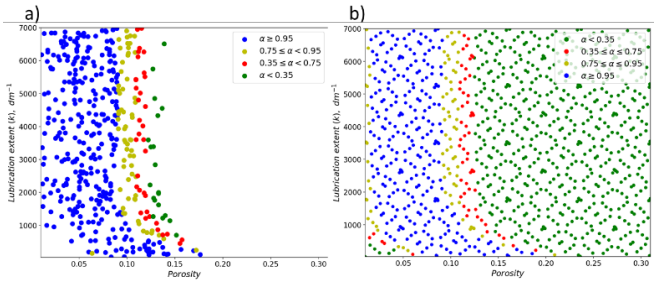

Figure 3. Probabilistic design space identified using (a) Nested sampling and (b) Quasi MCMC for the tableting process

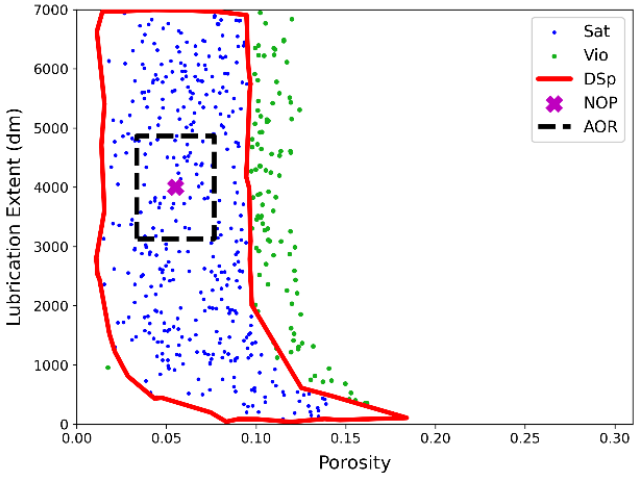

Figure 4. Acceptable Operating Region and Nominal Operating Point. 4

To visualize the AOR, probabilistic design space is segmented into satisfied (blue) and violated (green) regions, as shown in figure 4. The black line represents the AOR, encompassing the range of porosity and lubrication extent values that satisfy predefined constraints. The NOP, marked by a purple star at [0.055, 4000], serves as a reference for optimal system performance. The red line

indicates the DS boundary, beyond which the system may exhibit undesirable behavior. . A bisection search method is applied to expand a uniform square region outward from the NOP in all directions until one of the vertices reaches the boundary, ensuring that the AOR remains within acceptable design constraints. The final AOR size of 0.0625 dm^{-1}, derived from this iterative process, represents the largest feasible region centered around the NOP's lubrication extent and porosity values. This indicates improved process flexibility and robustness without violating constraints, providing a systematic approach to assess the system's operational limits under varying conditions.

4. CONCLUSION

This study successfully developed a probabilistic design space for a pharmaceutical tableting process using Bayesian inference and nested sampling. The approach effectively quantified and propagated uncertainties in model parameters, ensuring consistent tablet tensile strength (CQA) with over 95% reliability. The nested sampling method efficiently identified high-probability regions, reducing computational costs and enhancing precision. The acceptable operating range analysis demonstrated significant process flexibility and robustness. This work underscores the value of probabilistic DS in optimizing manufacturing processes and maintaining regulatory compliance, offering a powerful tool for consistent product quality and operational robustness. Future research will explore extending this methodology to other processes and parameters, with a focus on using iterative selection of nominal points to further explore process robustness and identify optimal operating conditions.

ACKNOWLEDGEMENTS

The authors acknowledge funding from the UK Engineering and Physical Sciences Research Council (EPSRC), for Made Smarter Innovation – Digital Medicines Manufacturing Research Centre (DM2), EP/V062077/1.

REFERENCES

1. Campbell, T. J. S.; Rielly, C. D.; Benyahia, B. Digital Design and Optimization of an Integrated Reaction-Extraction-Crystallization-Filtration Continuous Pharmaceutical Process. Comput.-Aided Chem. Eng. 2022, 51, 775–780.
2. Benyahia, B.; Brumano, L. P.; Pessoa, A.; Santos da Silva, F. V. Biopharmaceutical Development, Production, and Quality. In New and Future Developments in Microbial Biotechnology and Bioengineering: Microbial Biomolecules: Properties, Relevance, and Their Translational Applications; Elsevier, 2020; pp 69–89. https://doi.org/10.1016/B978-0-444-64301-8.00003-2.
3. Benyahia, B. Applications of a Plant-Wide Dynamic Model of an Integrated Continuous Pharmaceutical Plant: Design of the Recycle in the Case of Multiple Impurities. In Computer Aided Chemical Engineering; Elsevier B.V., 2018; Vol. 41, pp 141–157. https://doi.org/10.1016/B978-0-444-63963-9.00006-3.
4. Peterson, J. J.; Yahyah, M. A Bayesian Design Space Approach to Robustness and System Suitability for Pharmaceutical Assays and Other Processes. Stat Biopharma Res 2009, 1 (4), 441–449. https://doi.org/10.1198/sbr.2009.0037.
5. Peterson, J. J. A Bayesian Approach to the ICH Q8 Definition of Design Space. J Biopharm Stat 2008, 18 (5), 959–975. https://doi.org/10.1080/10543400802278197.
6. Bouchkira, I.; Benyahia, B. Multi-Objective Optimization Approach for Enhancing Flexibility of a Pharmaceutical Process. In Proceedings of the 34th European Symposium on Computer Aided Process Engineering / 15th International Symposium on Process Systems Engineering (ESCAPE34/PSE24), June 2-6, 2024, Florence, Italy; 2024; pp 1271–1278.
7. Lebrun, P.; Boulanger, B.; Debrus, B.; Lambert, P.; Hubert, P. A Bayesian Design Space for Analytical Methods Based on Multivariate Models and Predictions. J Biopharm Stat 2013, 23 (6), 1330–1351. https://doi.org/10.1080/10543406.2013.834922.
8. Tabora, J. E.; Lora Gonzalez, F.; Tom, J. W. Bayesian Probabilistic Modeling in Pharmaceutical Process Development. AIChE Journal 2019, 65 (11). https://doi.org/10.1002/aic.16744.
9. Sano, S.; Kadowaki, T.; Tsuda, K.; Kimura, S. Application of Bayesian Optimization for Pharmaceutical Product Development. J Pharm Innov 2020, 15 (3), 333–343. https://doi.org/10.1007/s12247-019-09382-8.
10. Yuan, X.; Benyahia, B. A Holistic Approach for Model Discrimination, Multi-Objective Design of Experiment and Self- Optimization of Batch and Continuous Processes. In Proceedings of the 34th European Symposium on Computer Aided Process Engineering / 15th International Symposium on Process Systems Engineering (ESCAPE34/PSE24), June 2-6, 2024, Florence, Italy; 2024; pp 391–396.
11. Kushner, J.; Moore, F. Scale-up Model Describing the Impact of Lubrication on Tablet Tensile Strength. Int J Pharm 2010, 399 (1–2), 19–30.

https://doi.org/10.1016/j.ijpharm.2010.07.033.
12. Nassar, J.; Williams, B.; Davies, C.; Lief, K.; Elkes, R. Lubrication Empirical Model to Predict Tensile Strength of Directly Compressed Powder Blends. Int J Pharm 2021, 592. https://doi.org/10.1016/j.ijpharm.2020.119980.
13. (Kushner IV, J. Incorporating Turbula Mixers into a Blending Scale-up Model for Evaluating the Effect of Magnesium Stearate on Tablet Tensile Strength and Bulk Specific Volume. Int J Pharm 2012, 429 (1–2), 1–11. https://doi.org/10.1016/j.ijpharm.2012.02.040.
14. Sachio, S.; Kontoravdi, C.; Papathanasiou, M. M. A Model-Based Approach towards Accelerated Process Development: A Case Study on Chromatography. Chemical Engineering Research and Design 2023, 197, 800–820. https://doi.org/10.1016/j.cherd.2023.08.016.
15. Benyahia, B.; Latifi, M.A.; Fonteix, C.; Pla, F. Emulsion copolymerization of styrene and butyl acrylate in the presence of a chain transfer agent. Part 2: Parameters estimability and confidence regions 2013, 90, 110–118. https://doi.org/10.1016/j.ces.2012.12.013.